Real-time assessment of three-dimensional cell aggregation in rotating wall vessel bioreactors *in vitro*

Gregory P Botta[1], Prakash Manley[2], Steven Miller[3] & Peter I Lelkes[1]

[1]Laboratory of Cellular and Tissue Engineering, Drexel University, New College Building, 245 N. 15th St., Philadelphia, Pennsylvania, USA. [2]Valleylab, Tyco Healthcare Group, Mail Stop A23, 5920 Longbow Drive, Boulder, Colorado 80301, USA. [3]I. Miller Precision Optical Instruments, Inc., 35 N. Second St., Philadelphia, Pennsylvania 19106, USA. Correspondence should be addressed to P.I.L. (pilelkes@drexel.edu).

Published online 14 December 2006; corrected online 4 January 2007 (details online); doi:10.1038/nprot.2006.311

Until now, tissue engineering and regenerative medicine have lacked non-invasive techniques for monitoring and manipulating three-dimensional (3D) tissue assembly from specific cell sources. We have set out to create an intelligent system that automatically diagnoses and monitors cell–cell aggregation as well as controls 3D growth of tissue-like constructs (organoids) in real time. The capability to assess, in real time, the kinetics of aggregation and organoid assembly in rotating wall vessel (RWV) bioreactors could yield information regarding the biological mechanics of tissue formation. Through prototype iterations, we have developed a versatile high-resolution 'horizontal microscope' that assesses cell–cell aggregation and tissue-growth parameters in a bioreactor and have begun steps to intelligently control the development of these organoids *in vitro*. The first generation system was composed of an argon-ion laser that excited fluorescent beads at 457 nm and fluorescent cells at 488 nm while each was suspended in a high-aspect rotating vessel (HARV) type RWV bioreactor. An optimized system, which we introduce here, is based on a diode pumped solid state (DPSS) green laser that emits a wavelength at 532 nm. By exciting both calibration beads and stained cells with laser energy and viewing them in real time with a charge-coupled device (CCD) video camera, we have captured the motion of individual cells, observed their trajectories, and analyzed their aggregate formation. Future development will focus on intelligent feedback mechanisms *in silico* to control organoid formation and differentiation in bioreactors. As to the duration of this entire multistep protocol, the laser system will take about 1 h to set up, followed by 1 h of staining either beads or cells. Inoculating the bioreactors with beads or cells and starting the system will take approximately 1 h, and the video-capture segments, depending on the aims of the experiment, can take from 30 s to 5 min each. The total duration of a specific experimental protocol will also depend on the specific cell type used and on its population-doubling times so that the required numbers of cells are obtained.

INTRODUCTION

Rotating wall vessel bioreactors

Rotating wall vessel (RWV) bioreactors have become a common low-shear culture venue for studying cellular aggregation and the formation of three-dimensional (3D) tissue-like assemblies (organoids). These organoids are demonstrably more differentiated, have increased size and exhibit behavior more similar to actual *in vivo* tissue than those cultured in either two-dimensional (2D) flasks or other bioreactors[1,2]. By mimicking natural tissue with higher fidelity, culture in RWV bioreactors permits more accurate evaluations of protein interactions, gene expression and signaling pathways[3–6]. The *in vitro* generation of these organoids recalls their ontogenesis *in vivo*, supporting the notion that RWV bioreactors might serve as suitable locations for *in vitro* embryology experiments. In regards to the mechanism of action of the RWV, the solid body rotation in the enclosed fluid medium allows cellular particles to be suspended continuously by the equalization of gravity-induced sedimentation against the constant upward forces provided by the rotation of the vessel[7]. Over time, the close proximity (colocation) of particles moving along with the fluid in the RWV facilitates the formation of cellular aggregates. These aggregates rapidly increase in size and mass, forming tissue-like assemblies, many of which can become up to three orders of magnitude larger than those in stationary flask cultures[8]. As they increase in mass, each organoid gains a more forceful gravitational pull on its structure, increasing shear stress and drag on the nascent tissue. So, without increasing the speed of rotation and offsetting the continually increasing gravitational pull, the organoids no longer remain in the venue-specific rotatory suspension culture as characterized by 'stationary' free-fall. Without appropriate and continual adjustment of the rotational speed, the growing cellular aggregates tumble and collide with one another, as well as with the walls of the RWV. The increasing collision frequency with the wall eventually results in the destruction of the nascent tissue-like assemblies. In current methodologies, the increase in velocity to perpetuate the continual free-fall of growing tissues has been manually or empirically coordinated from either past experience or from algorithmic knowledge of bodies tumbling in this environment[9].

Current techniques to determine aggregation kinetics in 3D

Past aggregation models have relied on inanimate particles or microcarrier beads seeded with cells in RWVs and have based their schemes on Smoluchowski's population-balance equations[10,11]. These current experimental procedures provide the 'real world' input for quantitative-aggregation models of microcarriers in RWVs, yet are confronted with the major disadvantage of static interference[9]. In other words, at each of the known or calculated time points during cellular aggregation, the bioreactor is regularly stopped and drained of its enclosed fluid medium in an effort to extract the growing cellular mass. After this step, the cellular body is studied for membrane linkages, measurement of its development and reaction to certain growth factors. Although these studies are well founded in their observational analysis, the developed tissue is often subjected to disruptive shear forces during the

deceleration and/or acceleration of the RWV as all vital measurements are determined in a stationary environment. In consequence, bioreactor studies have suffered from the inability to study cell–cell aggregation kinetics or organoid formation without disrupting the very tissue that is meant to be constructed.

Stationary techniques

In the past, the above procedures had been the only type of experimentation on cellular bodies in RWVs, mainly due to both optical and computerized imaging-technology limitations. A more recent approach to looking at cell aggregates used microparticles and validated the proposed numerical models by using a camera rotating in synchrony with a bioreactor[12]. Further studies implementing this rotating camera base have characterized and evaluated the movement and aggregation of bioceramic microcarrier beads in RWV cell cultures[13]. With a rotating frame of reference, these 'stationary' techniques were used to support the calculations of numerical models as well as to follow the mass-induced fluctuating trajectories of microparticles. However, these techniques neither assessed nor modeled the growth of cellular aggregates over time.

Dynamic techniques

With the improvement in optical hardware, as well as the advent of robust computerized analyses, storage capacities and transfer speeds, the opportunity to dynamically capture the real-time process of cellular tissue construction in the bioreactor without disruption has now been realized. Higher resolution imaging and the computational capability to analyze clearer microscopy images has opened the door for the development of our real-time imaging systems. In terms of outcomes, the primary long-term goal of this approach is to provide new tools for elucidating some of the crucial initial steps that lead from individual cells, through the formation of cell–cell aggregates, to the generation of functional multicellular tissue-like constructs. Also, we anticipate the development of suitable algorithms to translate parameters such as aggregate size, which is derived from the analysis of real-time images, into an effective feedback-control mechanism for the continual adjustment of the RWV rotational speed. This, in turn, will provide much needed automated and reproducible culture conditions in these bioreactors. Two versatile systems have been built so far, each incorporating the global characteristic of new real-time imaging analysis of diverse cell types in an RWV. The first system, built around an argon-ion laser, uses fluorescent calibration beads and carboxyfluorescein succinimidyl ester (CFSE) to stain PC12 and HepG2 cells[14]. The second system is a recently optimized assembly that provides a lower cost, more compact alternative, incorporating a diode pumped solid state (DPSS) frequency doubled green laser, rhodamine 6G Cytodex-2 calibration beads, and rhodamine 6G staining of various cell types.

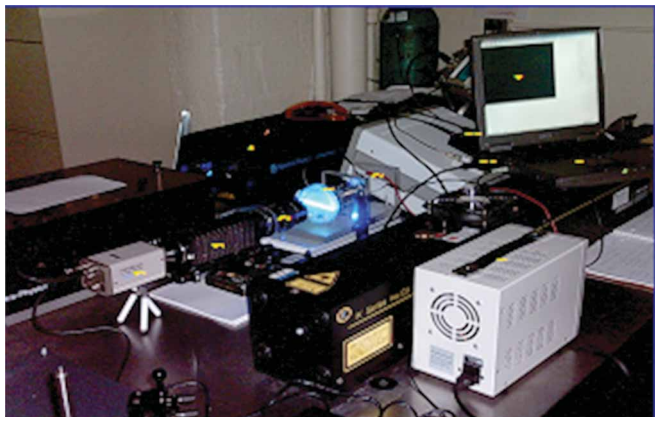

Figure 1 | The argon-ion laser system. The excitation and capture components of the system, as seen in their original mock-up.

Argon-ion gas laser system

As previously described[14], our new real-time cell-imaging system was developed to record and dynamically analyze cell trajectories and cellular aggregation in RWV bioreactors. In this particular (original) configuration, we used a tunable argon-ion laser (set at either 457 nm or 488 nm respectively) to laterally excite either the Fluoresbrite yellow–green polystyrene latex microsphere calibration beads or the CFSE-labeled cells suspended in a high-aspect rotating vessel (HARV), a specific type of RWV. Fluorescent images were captured with a charge-coupled device (CCD) video camera that was mounted in front of the clear front face of the HARV (**Fig. 1**). As each of these samples emits at distinct wavelengths, the emission filter had been adapted accordingly (for details, see MATERIALS). From the real-time imaging feed, a series of image frames were captured on a computer and analyzed for size distributions and aggregation kinetics.

Diode pumped solid state green-laser system

Following the initial validation of this prototype, we have optimized the system for global use, mainly through miniaturization and by cost reduction of the intrinsic components. Using state-of-the-art diode laser technology, we have designed an updated system that significantly reduces both cost economics for individual adaptability and weight for increased portability, while still embracing the tenets of the original argon-ion system (**Fig. 2**). Specifically, we now use a DPSS green laser that excites the rotating samples in the HARV through a dielectric mirror that provides a 90% transmission efficiency at a wavelength of 532 nm. With a CCD video camera, we have been able to optically capture high-resolution images ($<$ 10 μm) of both rhodamine 6G-labeled

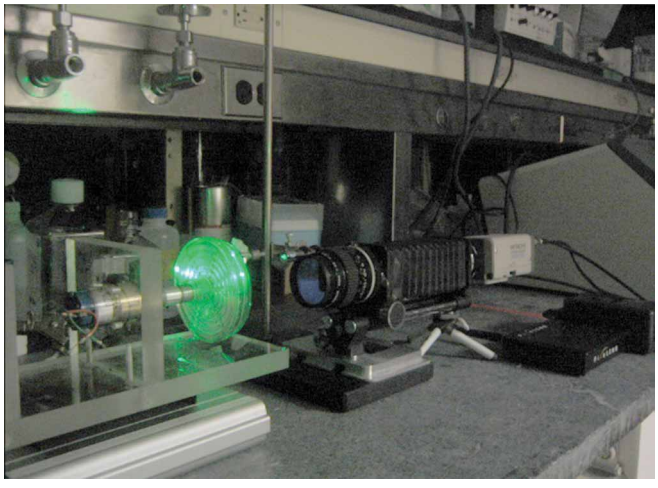

Figure 2 | The DPSS green laser system. A comparative view of the green laser system's reduced size and updated components in relation to the argon-ion laser system. DPSS, diode pumped solid state.

Dextran-based Cytodex-2 beads and PC12 cells suspended in the rotating HARV. Also, we are developing a new generation of image-analysis software that will incorporate a certain degree of automation into the system by capturing the original video signal, extracting its individual frames for input into a software program, and evaluating aggregate size as well as cellular composition.

Diversity of applications

These real-time horizontal microscopes are applicable to a wide range of processes, techniques and samples. Applications in our studies have included not only aggregation imaging and growth calculations, but also trajectory analysis of scaffolds, beads and cells for determining the optimal growth conditions of tissues in bioreactors (**Fig. 3**). The advantage of this system is that it can, in essence, non-invasively analyze the real-time assembly or disassembly kinetics of fluorescent objects that are as small as ~ 4 μm in diameter (for example, a human lymphocyte that was cultured in a dynamic venue such as the RWV; P.M., Donald M. Simons and P.I.L., unpublished observations). In the past, when studying the assembly of chondrocytes, cancer cells, or cells of neuronal origin, only static approaches were available to tediously evaluate aggregation kinetics[3,15–17]. In the future, our approach will be useful for assessing aggregation kinetics of different cells through an artificial, computer-aided feedback algorithm that will recognize organoid size, adjust the RWV speed to support the continual free-fall (simulated microgravity) environment, and thereby increase nascent-tissue formation.

Experiments that use this technology could provide a real-time analysis of the formation of embryoid bodies (EB) from embryonic stem cells[18]. With standardized organoid-growth conditions, high-throughput generation and screening of these EBs becomes a possibility. As the EBs and other cell aggregates are being formed and begin to grow in a HARV, antibodies can be applied to the growth media and mechanistic studies of their effects can be recorded. So, our existing system will allow one to observe the effects of exogenously added growth and adhesion factors on the creation of 3D organoids in real-time. Indeed, we have already begun to do so in studying aggregation characteristics of highly aggressive metastatic cancer MDAMB231 cells, compared with lowly aggressive, non-metastatic cancer MCF7 cells (G.P.B. and Alexandra Vamvakidou, unpublished results). Also, with sufficient resolution, the system will allow the use of proliferation-specific dyes for visualizing differentiation and growth during *de novo* tissue formation. As a final example, using multicolor-staining complexes and multiwavelength-emission filters, our system will allow real-time continual monitoring of the generation of heterotypic tissue-like constructs in 3D. Importantly, as organoids constructed in bioreactors have characteristics more closely resembling those of native tissues, complex constructs grown in this automated environment would serve as improved cellular models for drug discovery and drug testing, as compared with the current static, 2D tissue models.

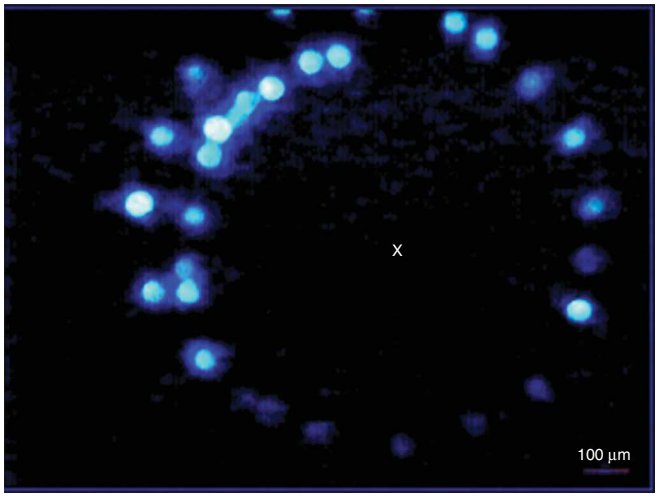

Figure 3 | Time-lapsed trajectory imaging. Thirty individual frames have been superimposed on one picture presenting the trajectory composition of a rotating microsphere in the high-aspect rotating vessel (HARV). The center of the trajectory is marked with an X[25].

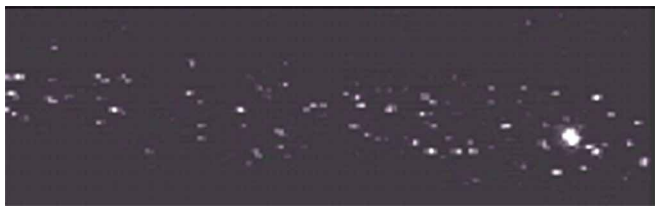

Figure 4 | Increased field of view limitations. Due to decreased magnification and resolution of the sample caused by an increase in the width of the field of view (FOV), a balance must be achieved between the number of particles that can be viewed at each frame and the precise visualization of individual particles.

Limitations

A major limitation of these imaging systems is the limited field of view (FOV) that is obtained by the CCD video camera while capturing images of the HARV. Increasing the FOV to accommodate either large aggregates or an increased analysis area results in a reduction in the magnification of the system. With the resolution and available light sensitivity of the current camera, a reduction in magnification would not appropriately permit the evaluation of single cells or doublet aggregates (**Fig. 4**). As the best optical resolution for our camera is 2.34 μm per pixel in a FOV of 1.5 mm by 1.125 mm at a working distance of 5.5 cm, this system works well for microspheres of roughly 20 μm, and cells of around > 8 μm in diameter within a radius 1–2 cm from the center of the HARV. With these constraints, we can still discern the formation of organoids of ~0.75 mm in diameter and can discern individual cells in these multicellular aggregates. A low-light, high-magnification camera should be able to capture a wider FOV while still distinguishing such small tissue aggregates.

Duration of exposure to the fluorescent excitation by the laser is a limitation to continual long-term studies, as photobleaching of the fluorophore and photodynamic damage of the cells are common problems in fluorescence microscopy. Short, intermittent excitation (from 30 s to 5 min) did not result in photobleaching of the Fluoresbrite yellow–green beads, rhodamine 6G stained beads and cells, or CFSE stained cells, but continuous irradiation for 10 min or more caused bleaching of the Fluoresbrite yellow–green beads and CFSE stained cells at the center of the HARV. By contrast, we found rhodamine 6G to be significantly more resistant to photodegredation. The central localization of photobleaching was due to the continual irradiation near the center of the HARV,

whereas radial areas spent only a moment in the beam's energy. Similarly, extended exposure to the high-energy laser that is needed to visualize the samples in real-time applications might have phototoxic effects at increased power. In our hands, excitation at 35 mW did not impair the viability of the cell for up to 24 h after excitation.

Future advancements

As indicated above, we have begun to automate the image-processing routines in order to satisfy three aims in creating an intelligent feedback mechanism for dynamic, self-directed tissue growth. The first aim is to automate the image-extraction steps in an effort to separate individual frames from the original video feed, whereas the second aim is to automate the analysis of these individual frames using custom-built software. We will use an open-source C++ image-analysis software library to extract the number of aggregates formed, the size of each aggregate, and the number of individual cells comprising each aggregate from each image. The third aim in the feedback circuit will be to use the information obtained from the images for controlling the rotational speed of the RWV so that as the mass of the aggregates increases or decreases, the stepper motor in the HARV base will increase or decrease the rotational speed of the HARV. This will enable us to automatically maintain the 'continual free-fall suspension' (simulated microgravity) condition that is necessary for the consistent formation of 3D organoids.

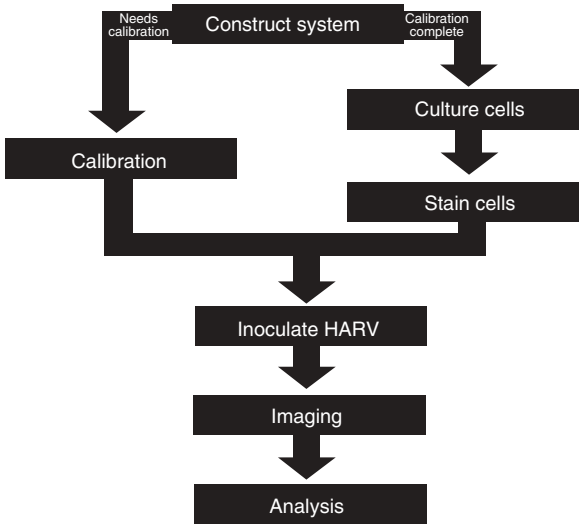

Figure 5 | Overall procedure flowchart. A graphical representation of the necessary and optional steps of the experimental protocol. HARV, high-aspect rotating vessel.

Flow diagram

A flow diagram of the entire procedure is presented in **Figure 5**. See **Figure 6** for a timeline.

MATERIALS

REAGENTS

- Dulbecco's modified eagle's medium (DMEM, Cellgro, cat. no. 10-013-CV) (see REAGENT SETUP)
- L-glutamine (Sigma-Aldrich, cat. no. G-3126)
- Glucose (Sigma-Aldrich)
- Fetal bovine serum (FBS, Clontech)
- Horse serum (HS, Clontech)
- Minimal essential medium (MEM, Cellgro, cat. no. 10-010-CV) (see REAGENT SETUP)
- Penicillin–Streptomycin (Sigma-Aldrich)
- Real-time Dulbecco's modified eagle's medium (RT-DMEM, Sigma-Aldrich, cat. no. D2906) (see REAGENT SETUP)
- Sodium pyruvate with pyridoxine hydrochloride (Sigma-Aldrich)
- Real-time minimal essential medium (RT-MEM, Cellgro, cat. no. 17-305-CV) (see REAGENT SETUP)
- PC12 rat adrenal pheochromocytoma cells (Gordon Guroff, National Institutes of Health (NIH), cultured as described in P.I.L. and Brian R. Unsworth, 2006)
- HepG2 human hepatocellular liver carcinoma cells (ATCC, cat. no. HB-8065)
- 0.1 N sodium hydroxide (NaOH) for the sterilization of the bioreactor (Sigma-Aldrich)
- Carboxyfluorescein succinimidyl ester, CellTrace CFSE Cell Proliferation Kit for argon laser microscope (Invitrogen, cat. no. C34554)
- Pure Rhodamine 6G for green DPSS laser microscope (Acros Organics, cat. no. 191410500)
- Trypsin (Sigma-Aldrich)
- HEPES (4-(2-hydroxyethyl)-1-piperazineethanesulfonic acid, Cellgro, cat. no. 25-060-C1)

EQUIPMENT

- Micro-Nikkor 55 mm f/2.8 macro lens (Nikon)
- Bellows unit to increase optical magnification to 4 × and the electronic magnification to 120 × (Nippon Kogaku, cat. no. 94809)
- FireWire video converter to convert the coaxial analog signal to FireWire standard by peripheral data transmission with a 1394 6-pin at 400 megabits per s (PixeLINK, cat. no. PL-A544)

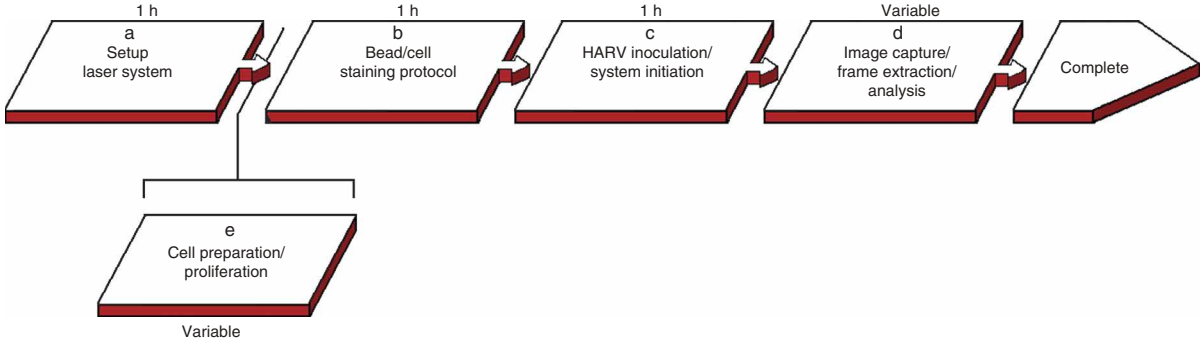

Figure 6 | Protocol timeline. A timeline that estimates the time necessary for each step of the protocol. Steps d and e will vary in time depending on the needs of the experiment. Also, step e should be included when running the real-time analysis of cells and is not necessary if only calibrating the system with beads. HARV, high-aspect rotating vessel.

- 12-V DC adapter for Hitachi CCD (Zachariah & Lundbergh Inc., cat. no. HES20-11)
- 12-V DC adapter for PixeLINK FireWire converter (RadioShack)
- VirtualDub v1.6.15, free program licensed under General Public License (GNU) that is used for video capture and processing on all Windows platforms (VirtualDub)
- NIH ImageJ, open source image analyzer used for measurements of size and number (NIH)
- ImagePro Plus 5.0, licensed software used for 2D and 3D image processing and enhancement as well as numerical analysis with extensive measurement and customization features (Media Cybernetics)
- Background subtraction toolkit, free Java software tool that removes any remnants of the excitation source from the background of an image (Olympus, http://www.olympusmicro.com/primer/digitalimaging/backgrounddownload.html)
- 0.5-inch diameter visible dielectric mirror, a high-reflectance mirror that transmits energy from 450–700 nm and has a 1 J per cm^2 damage threshold (New Focus, cat. no. 5151)
- 0.5-inch corner mount, a mirror mount that allows tilt, tilt without translation and pure translation for varying the illumination and observation angles (New Focus, cat. no. 9808)
- 20-µm cell sieve (Fisher Scientific)
- Corning T-175 flasks (Sigma-Aldrich, cat. no. 431080)
- 0.5-inch charge-coupled device (CCD) color video camera, incorporating 768 × 494 pixels for an NTSC (National Television Standard Committee) system, a RGB/YC connector, and a BNC (Bayonet–Neill–Concelman) video connector (Hitachi Denshi America, cat. no. KP-D50)
- Rotary cell culture system (RCCS-D, Synthecon Inc., Houston, Texas) (see EQUIPMENT SETUP)
- 27-V DC gear motor (Motor Technology Inc., cat. no. 126A190)
- 0–30-V DC (0–3 A) regulated DC power supply (Circuit Specialists, Inc., cat. no. CSI3003X)
- 50-mL Bioreactor high aspect rotating-wall vessel (HARV, Synthecon Inc.)
- Argon-ion laser, an industrial small frame laser that emits a multiline 1.7-mm diameter beam over a range of output powers with a beam lock for stability between uses (BeamLok 2060-7S, Spectra-Physics)
- Fluoresbrite yellow–green fluorescent polystyrene latex microspheres (Polysciences Inc., packaged as 2-mL vials of 2.5% solids in water at sizes of 20 µm (cat. no. 19096-2), 45 µm (cat. no. 18242-2) and 90 µm (cat. no. 18243-2) that excite at 457 nm and emit at 486 nm)
- 486-nm bandpass filter calibration beads (Omega Optical)
- 517-nm cutoff filter (Omega Optical)
- Diode pumped solid state (DPSS) green laser (MBP BiggieLasers)
- Cytodex-2 microcarrier beads (Sigma-Aldrich, cat. no. C0646)
- 545-nm ALP filter (Omega Optical)

REAGENT SETUP

Dulbecco's modified eagle's medium (DMEM) Supplement with 2 mM L-glutamine, 4.5 g per L glucose, 7.5% FBS and 7.5% HS.

Minimal essential medium (MEM) Supplement with 10% FBS and 1% Penicillin–Streptomycin.

Real-time Dulbecco's modified eagle's medium (RT-DMEM) Supplement with 110 mg per L sodium pyruvate with pyridoxine hydrochloride, 2 mM L-glutamine, 7.5% FBS, 7.5% HS, and without phenol red.

Real-time minimal essential medium (RT-MEM) Supplement with 110 mg per L sodium pyruvate with pyridoxine hydrochloride, 10% FBS, and without phenol red.

EQUIPMENT SETUP

A current (2006) high-end computer running Windows XP ! CAUTION It is recommended that the computer be equipped at the minimum with a solo processor capable of 3.0 GHz or a dual processor capable of at least 1.73 GHz, 1 GB RAM, an 80 GB hard drive, and a FireWire port. Helpful additional accessories would include an external hard drive with a 250 GB storage capacity as well as a monitor capable of at least 1280 × 800 pixels. ! CAUTION Certain computer components such as processor speed, RAM hard drive capacity, and a FireWire port are absolutely necessary for acquiring and processing high-speed high-resolution images in real time.

Rotary cell culture system (RCCS-D) A package consisting of a rotator base, power supply, and four 50-mL disposable HARVs. Alternatively, for economic reasons, you can build your own simple, custom-designed rotator base. The base used for these protocols was constructed at the Drexel University, Philadelphia, Pennsylvania, USA, machine shop with a 27-V DC gear motor for turning the custom rotator base and a 0–30-V DC (0–3 A) regulated DC power supply to power the motor for the custom rotator base.

50-mL bioreactor High-aspect rotating-wall vessel (HARV) ! CAUTION A 10-mL disposable HARV is not suitable for this protocol as the luer lock ports on the front face are spaced too closely for the CCD magnification capabilities, disrupting the FOV and the line of sight needed for proper imaging.

Argon-ion laser microscope equipment For calibration beads: 486-nm Bandpass filter, a 52-mm threaded filter with 85% transmission efficiency and a full-width half-maximum of 20 nm. For CSFE stained cells: 517-nm Cutoff filter, a 52-mm threaded filter with 87% transmission efficiency and high attenuation levels below 500 nm.

DPSS green laser microscope equipment DPSS green laser. For both rhodamine 6G-stained calibration beads and cells: use a 545-nm ALP filter, a 52-mm threaded, long-pass filter with a cut-on wavelength at 545 ± 2 nm that transmits from 547 nm to the far IR region at 80–90% transmission. The filter's blocking region includes UV-visible to 532 nm. ! CAUTION We used a high power IR laser diode that, at 808 nm, pumps a tiny block of ND:YVO_4 (neodymium doped yttrium orthovanadate) generating light at a wavelength of 1,064 nm. That light feeds a potassium titanium oxide phosphate (KTP) intracavity frequency doubled crystal to produce the green beam at 532 nm[19].

Cytodex-2 microcarrier beads Inanimate cell analogs, Dextran beads supplied in a suspension of 0.9% saline with positive-charged DEAE (diethylaminoethyl) groups throughout matrix. ▲ CRITICAL Prior to use, swell beads in PBS (50 mL per g) and autoclave at 120 °C for 20 min.

PROCEDURE

Construction of horizontal microscopes

1| Select the laser–stain combination that is most adaptable to your current experiment, either argon-ion laser and CFSE or the DPSS green laser and rhodamine 6G.

2| Following the schematic (**Fig. 7**), obtain the proper working distance (5.5 cm) by attaching the empty 50-mL RWV to the rotator power base. If the rotator base was custom built, set the 0–30-V DC power supply to 27-V DC and connect it to the motor of the rotator base.

3| To set up the CCD video camera, attach a bellows unit to the camera lens' f-adapter and extend the bellows unit to its maximum length. Attach the 55-mm Nikon macro lens to the end of the bellows unit closest to the HARV. Connect the camera's coaxial output to the PixeLINK FireWire converter and connect the PixeLINK FireWire to the computer's 1394 standard adapter. Now, connect both the camera's and the PixeLINK's 12-V DC power supplies. Set the shutter speed at 4 ms for microspheres and 10 ms for cells.

▲ CRITICAL STEP Be sure to set the camera up so that the lens is at a working distance of 5.5 cm from the front face of the HARV.

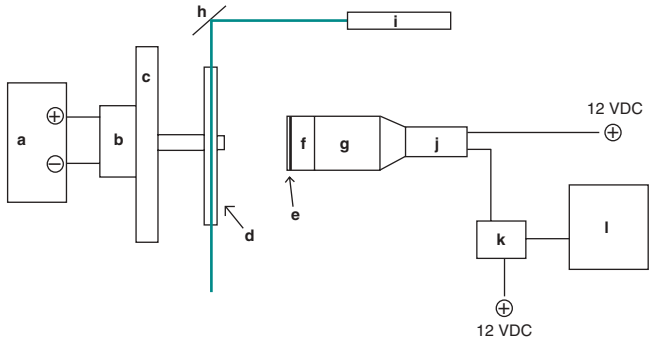

Figure 7 | The DPSS green laser system schematic. The green laser system is consists of an excitation source, an optical capturing equipment, experimental equipment and a power sources. (**a**) A 0–30-V DC power source. (**b**) A 27-V DC motor. (**c**) A custom high-aspect rotating vessel (HARV) rotator base. (**d**) A 50-mL HARV. (**e**) An optical emission filter. (**f**) A macro lens. (**g**) A bellows unit. (**h**) A high-reflectance mirror. (**i**) A DPSS (diode pumped solid state) double frequency green laser. (**j**) A charge-coupled device (CCD) camera. (**k**) A PixeLINK analog to digital converter. (**l**) A high-performance computer. The green line represents the trajectory of the laser from source to output.

4| Place the specific laser behind the bellows unit's lens at a level just above the plane that is bisected by the center of the HARV (**Fig. 7**).

! CAUTION Both lasers operate at wattage described as a class IIIa safety level and may damage your eyes with extended or magnified use. Use proper personal protective equipment (i.e., safety glasses).

▲ CRITICAL STEP Placement of the laser behind the bellows unit's lens will help reduce any background illumination caused by the laser's light during imaging (**Fig. 7i**).

? TROUBLESHOOTING

5| Mount the precision mirror at a 45° angle, at the same height as the laser such that when the beam is reflected, it bisects the HARV.

■ PAUSE POINT Following the construction of the horizontal microscope system, the system can be left indefinitely until experiments are started.

? TROUBLESHOOTING

HARV calibration preparation

6| Calibrating the imaging system requires preparation of either Fluoresbrite yellow–green fluorescent polystyrene latex microspheres for the argon-ion laser (A) or rhodamine 6G stained Cytodex-2 beads for the DPSS green laser (B):

(A) Calibration with Fluoresbrite yellow–green fluorescent polystyrene latex microspheres for the argon-ion laser.

(i) Depending on the microsphere size (20 μm, 45 μm, 90 μm) and based on the manufacturer's concentration, create 60-mL aqueous suspensions containing between 2×10^5 and 1×10^6 particles per mL of distilled H_2O, as based on established seeding densities in HARVs[20,21].

(ii) Follow the HARV inoculation procedure (Step 16).

(B) Calibration with rhodamine 6G stained Cytodex-2 beads for the DPSS green laser.

(i) Create a solution of 3 mg per mL rhodamine 6G in distilled (cell-culture grade) water.

(ii) Add 5 μL of the rhodamine 6G solution to 10 mL of bead suspension for a final concentration of 1.5 μg rhodamine 6G per mL of solution and incubate for 10 min.

(iii) Pellet (2 min at 800 r.p.m (50*g*), at room temperature (RT, 25 °C) and resuspend in distilled water three times for a final suspension (in 60 mL) at a concentration of 1×10^6 beads per mL.

(iv) Follow HARV inoculation procedure (Step 16).

Cell culture

7| For cell aggregation with HepG2 or PC12 cells, thaw frozen cells and place them into a T-175 flask with 20 mL of prewarmed (37 °C) media, using established cell-culture procedures[20,21].

▲ CRITICAL STEP All cell handling must be carried out under aseptic conditions in a biological safety cabinet, as per established cell-culture procedures.

8| Place cells in a temperature- and CO_2-regulated incubator (37 °C, 5% CO_2) and culture them using established techniques.

! CAUTION For PC12 cells, which grow in clumps, do not let the cells grow > 50% in confluence prior to passaging. For HepG2 cells, split the cells as they reach confluence but do not let any culture become over confluent.

9| After you have grown the cultures to have enough cells for your experiments (and for continuing the cell culture for repeat studies), harvest the cells by aspirating and discarding the culture medium.

10| Briefly rinse the cell layer with Ca^{2+}- and Mg^{2+}-free PBS, then aspirate.

11| For PC12 cells, gently tap the flask to dislodge the cells. For HepG2 cells, follow standard procedures for trypsinization. Add 1.0–2.0 mL of trypsin–EDTA solution to the flask, and observe cells under an inverted microscope until the cell layer is dispersed (usually within < 1 min).

! CAUTION To avoid clumping, do not agitate the cells by hitting or shaking the flask while waiting for the cells to detach.
! CAUTION Do not let the cells become over confluent, at which time they will be difficult to remove by trypsinization. If this should occur, reculture a new batch of cells.

12| Add 6.0 to 8.0 mL of complete DMEM medium to quench the trypsin. Remove the cells by gently pipetting and centrifuge at 800 r.p.m. (50*g*) for 5 minutes at RT.

13| After centrifugation, aspirate the supernatant and resuspend the cells in 1 mL of RT-DMEM. Count and aliquot the cells such that you obtain 60 mL of cell suspension at 1×10^6 cell per mL for the 50 mL HARV.
▲ CRITICAL STEP Any concentration of less than 2×10^5 cells per mL will create an environment of singlet cells that, without cell contact, rapidly undergo apoptosis. Any concentration greater than 5×10^6 cell per mL will yield large aggregates (especially for HepG2 cells) that can range in size from 5–10 mm in diameter within 4–6 h. These large aggregates rapidly deplete the HARV nutrients and form necrotic cores.
? TROUBLESHOOTING

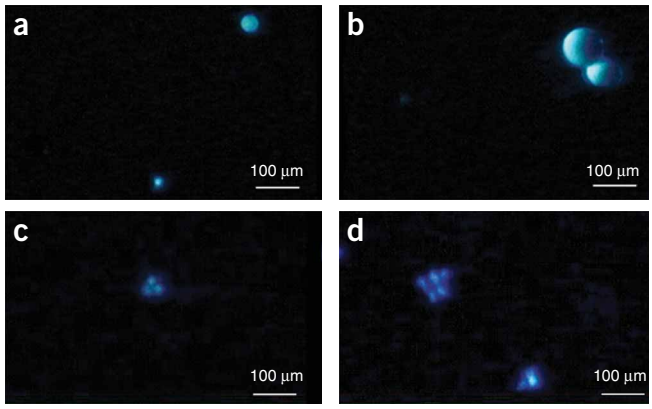

Figure 8 | Imaging of stained fluorescent microspheres and PC12 cells. (**a**) Two individual microspheres. (**b**) A microsphere doublet. (**c**) A single multicellular aggregate. (**d**) Two multicellular aggregates[25].

Cell staining for real-time analysis

14| Pellet the cell suspension at 800 r.p.m. (50*g*) for 5 min at RT, and resuspend at 1×10^6 cells per mL in prewarmed (37 °C) PBS containing either CFSE (5 mM in complete DMEM) for the argon-ion laser (A) or rhodamine 6G (1.5 μg per mL in complete DMEM) for the DPSS green laser (B).

(A) Staining with 5 mM CFSE for the argon-ion laser.

(i) Incubate the cells for 15 min and then repellet and resuspend in fresh prewarmed RT-DMEM.
(ii) Incubate the cells for 30 min and then repellet and resuspend in 60 mL of fresh prewarmed RT-DMEM at a concentration of 1×10^6 cells per mL.

▲ CRITICAL STEP Recommended concentration is 0.5–25 μm peaking at 492 nm and emitting maximally at 517 nm. However, these concentrations lead to rapid photobleaching, so we used concentrations of 5 mM. Optical properties are altered due to formation of dimers and higher aggregates that result in a more photostable and visibly enhanced emission at 517 nm[22]. Preliminary experiments show that this concentration did not impair normal aggregation process, was not cytotoxic, and did not impair cell proliferation. The cells retained fluorescence in a T-flask for at least two passages.
! CAUTION In our hands, 585-nm quantum dots (Quantum Dot Corporation) and CellTracker CM-DiI (Molecular Probes, cat. no. C-7001), although possessing unique optical properties such as high quantum yields and little or no photobleaching, did not work as well due to non-uniform, punctuate labeling of the cells. This factor leads to poor edge detection by the CCD video camera and poor analysis by the software.

(B) Staining with rhodamine 6G for the DPSS green laser.

(i) Create a solution of 3 mg rhodamine 6G to 1 mL of water.
(ii) Add 5 μl of the rhodamine 6G solution to 10 mL of cell suspension (in serum-free DMEM) for a final concentration of 1.5 μg rhodamine 6G per mL of solution, and incubate for 10 min.
(iii) Repellet at 800 r.p.m. (50*g*) for 5 min at RT and resuspend in fresh prewarmed complete RT-DMEM three times for a final suspension of 60-mL RT-DMEM at a concentration of 1×10^6 cells mL.

15| Prior to inoculation, pass the stained cell suspensions through a 20-μm sieve to filter out only singlets for initial experimental time points and follow the HARV inoculation procedure (Step 16).

HARV inoculation procedure

16| Using aseptic techniques, holding the HARV upright at a ~ 45° angle with two syringes (plungers removed) attached to the top and bottom luer lock ports, fill the vessel with the cell suspension or calibration beads through the HARV's lower syringe (luer lock port)[20,21]. The empty syringe attached to the upper luer lock will serve as the receptacle for the excess medium (or cell suspension) after complete filling of the HARV.
▲ CRITICAL STEP It is imperative that all air bubbles are removed from the HARV assembly prior to operation. Any residual bubbles will negate the principle of complete solid-body rotation, interfere with consistent cell aggregation, and impair organoid formation.
▲ CRITICAL STEP Initially filling the 50-mL HARV with 60 mL creates the reservoir overflow suspension needed to fully fill the HARV. However, be sure that only 50 mL of suspension is added as not to damage the HARV's internal membrane.
? TROUBLESHOOTING

17| Upon complete filling of the HARV, close the luer locks, remove the syringes, and sterilize the top plastic face of the HARV with 70% ethanol. Cap the luer lock inlet ports to prevent leakage and contamination.

18| Firmly screw the HARV onto the rotator base and start the rotation at a speed of 10 r.p.m.

19| Place the HARV and cells in a temperature and CO_2 controlled incubator (37 °C, 5% CO_2) during periods when imaging is not necessary. During periods of imaging, the HARV can be removed for 30 min without loss to cell viability due to pH changes. The longest time we have run a HARV has been for 20–30 days, but in this imaging system our longest interval was a maximum of 24 h.

▲ **CRITICAL STEP** Since the viability of cells outside of an environmentally controlled incubator is largely based on maintaining physiological pH characteristics, use appropriate discretion. It may be necessary to increase the buffer capacity by including 25-mM HEPES to the culture medium[20]. Additionally, should cells die or disintegrate in the HARV during imaging or incubation periods, their fluorescent signals will be lost to the environment and could, in theory, create increased background in the medium, although we have not witnessed this phenomenon. Cells that do not aggregate will subsequently die by anoikis; apoptotic lysis reduces their mass and, therefore, they will not interfere with the live-cell trajectory.

? TROUBLESHOOTING

■ **PAUSE POINT** The HARV can be left in the incubator for extended periods when loaded with a concentration of 1 million HepG2 or PC12 cells per mL. However, the cell media must be refreshed once a day by manual removal and refilling[21].

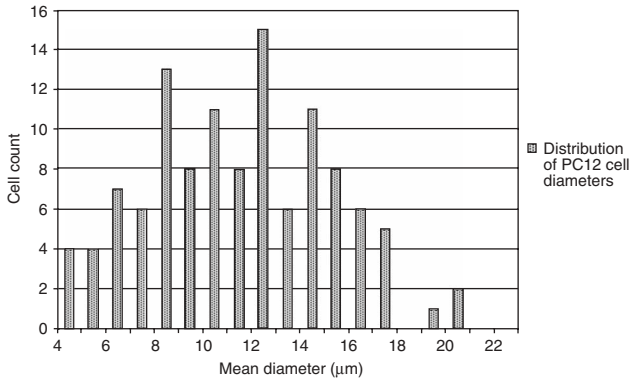

Figure 9 | PC12 calculated diameters. A graph depicting the calculated diameters of PC12 cells by frame-extracted-image analysis while in the rotating wall vessel (RWV) bioreactor. The measurements confirm published values (Fujita, 1989)[24].

Imaging procedure

20| With the CCD video camera turned on, the PixeLink converter operational, the laser activated and the HARV rotating at 10 r.p.m. open the VirtualDub software package on your computer.

? TROUBLESHOOTING

21| Click 'File' > 'Capture AVI'. This will take you into 'Capture Mode'.

22| Click on 'Video' > 'Source' and choose your camera input device. Also select the video standard as NTSC and press 'OK'.

23| Next, choose the correct format you would like the video to be captured in by clicking on 'Video' > 'Format'. Change the capture format to 24-bit and the image size to 640 × 480 (or larger depending on your hard drive space and monitor specifications) and press 'OK'.

24| Choose the number of pictures taken per s by adjusting the frame rate. Choose 'Capture' > 'Settings' and select the appropriate frame rate for your camera. When you are finished press 'OK'.

▲ **CRITICAL STEP** Using a 30 frames per s camera on a 1.87 G Hz dual-processor computer with 1 GB of RAM, we were able to adequately capture pictures up to 1 cm from the radius of the HARV's center. Slower frame rate cameras will be restricted to the HARV's center for analysis, whereas 100 frames per s cameras could theoretically capture the entire radius of the HARV.

▲ **CRITICAL STEP** Increasing the frame rate increases the file size; be sure to have adequate hard drive space, as a 1 min recording of high-resolution images at a rate of 30 frames per s requires approximately 1 GB of memory.

? TROUBLESHOOTING

25| Set the compression of the capture by selecting 'Video' > 'Compression'. Set it to 'uncompressed' to obtain the highest quality images for analysis and press 'OK'.

26| Next, create a location and file name for the video to be captured by choosing 'File' > 'Set Capture File'. Select a name and location to save the file and press 'OK'.

27| Begin recording your video images by selecting 'Capture' > 'Capture Video'. Many of our videos span only 30–60 s to accommodate limited hard drive space on the laptop, as each min of video uses ~1 GB of memory. When you finish recording, press 'Escape' to terminate the program.

? TROUBLESHOOTING

28| Choose 'File' > 'Exit Capture Mode' to return to the VirtualDub home screen.

■ **PAUSE POINT** After the images have been captured and saved, the frame-extraction procedure can start at any time.

Frame-extraction procedure

29| In VirtualDub, open your saved video by choosing 'File' > 'Open Video'.

30| Each frame will be placed in sequence in the display window. By moving the slider below the display window, you can choose specific frames to view. When you would like to extract a specific frame from the video, note its frame number and go to 'Video' > 'Select Range'. For the 'Start Offset' field, type in the frame you want to save in the right hand box. Then type in how many frames past that one you would like to save in the right hand 'Length' box. If you just want to save that one frame, type a '1' for 'Length' and click 'OK'.

31| Now choose 'File' > 'Save Image Sequence'. Type a prefix name to be appended to each image and an appropriate directory and folder to save your images. Select your output image as BMP, TARGA, or JPEG and press 'OK'. Your frames will then be extracted and saved in the specified location.

? TROUBLESHOOTING

■ **PAUSE POINT** After the frames have been extracted, their analysis can be done at any time.

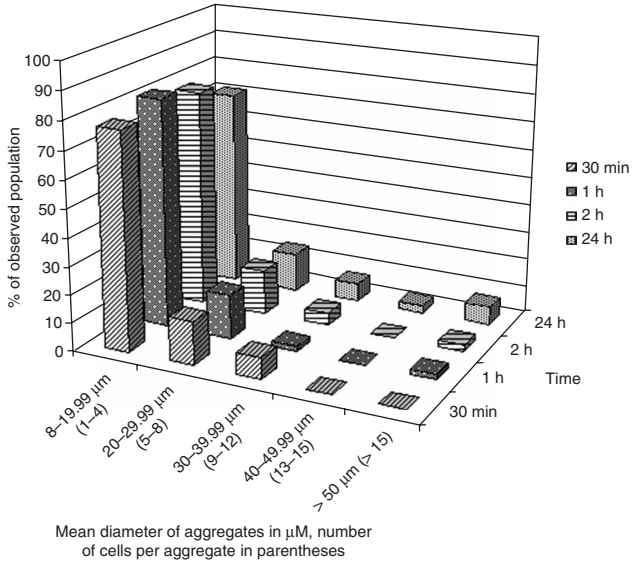

Figure 10 | PC12 cell aggregation over time. A graphical representation of the aggregation diameters of specific PC12 cells over a 24-h period as calculated by images retrieved from the laser systems[24].

Analysis procedure

32| For the image-analysis procedure, open an analysis program such as ImageJ or ImagePro Plus 5.0.

33| Select 'File' > 'Open', find the specific location of your saved frames, and click 'Open'.

34| Use measurement, imaging and thresholding techniques on your extracted frames following NIH documented protocols[23]. Each of these chronologically extracted frames can be used in endpoint-comparison sampling.

● **TIMING**

A timeline of the entire procedure is presented in **Figure 6**.

? TROUBLESHOOTING

Troubleshooting advice can be found in **Table 1**.

TABLE 1 | Troubleshooting table.

Problem	Possible reason	Solution
The CCD video camera is not capturing images	Camera power is 'OFF'	Plug in and turn on camera
	Camera connection to 12-V DC is not properly attached	Detach and reattach connection
	Camera connection to PixeLINK is not properly attached	Detach and reattach connection
	The PixeLINK is not properly attached to the computer	Detach and reattach connection
	The proper lens filter is not attached	Check that filter is appropriate for laser wavelength
	The media contains phenol red	Change media of HARV to that containing no phenol red
The computer image is blurred	The camera lens is not focused	Focus the lens by rotating counter clockwise and/or clockwise
	The camera lens is not properly distanced from the HARV	Space the lens an appropriate working distance from the HARV, based on shutter speed and HARV rotational speed
	The camera shutter speed is incorrect	Be sure that the shutter speed has been set properly depending on the HARV r.p.m. and FOV

TABLE 1 | Troubleshooting table (continued).

Problem	Possible reason	Solution
	The cells are not stained correctly	Follow cell-staining protocol, making sure to consult additional references and book chapters cited
	The rhodamine 6G beads are not stained correctly	Follow bead-staining protocol
	The media contains phenol red	Change media of HARV to that containing no phenol red
The computer image is too dark	The software is not properly brightening the image	Adjust the brightness setting in the software
The sample is indistinguishable on the computer screen	The background light is too bright	Adjust the brightness setting in the software
	The software is not properly contrasted	Adjust the contrast setting in the software
The HARV contains bubbles	The HARV was not inoculated properly	Follow the protocol for HARV inoculation. If necessary, fill and empty the HARV in an oscillatory manner through the upper and lower points. Also, consult the references and book chapters cited in the text
	The HARV does not have positive pressure	Inoculate the HARV again with 1 mL more cell suspension than the HARV requires
The HARV is not rotating	The motor is not connected to the power source	Reconnect the motor to the power source being sure that charges are matched correctly
	The power source is not set to 27-V DC	Reset the power source to the correct voltage and current
	The HARV is not properly attached to the base	Be sure to screw the HARV onto the rotator base
There are no aggregates after running the experiment	The number of cells prepared was below 2×10^5 cells per mL	Count the cells again and be sure to prepare the proper cell to media ratio in the suspension
	The HARV is rotating too quickly, driving the aggregates against the HARV wall	Reduce the speed of the HARV during the experiment, being sure that the cells were passed through a sieve prior to inoculation
	The cells were not initially viable	Be sure the cells are proliferating, validating their viability
	The cells have been removed from the incubator too long	Be sure to either create an experiment that does not deteriorate the viability of the cell or place the system in an incubator
	The cell medium has expired or is contaminated	Be sure to check the expiration date of the medium and its effect on cell proliferation
The aggregates are too large after running the experiment	The number of cells prepared was greater than 5×10^6	Count the cells again and be sure to prepare the proper cell to media ratio in the suspension
	The cells were not initially passed through a sieve before inoculation	Pass the cells through a sieve before inoculation, reducing the initial aggregates from the bioreactor
The computer cannot save the images on the hard drive	There is no free space on the hard drive	Delete unneeded files from the hard drive or upgrade the computer's hard drive space
The software does not open on the computer	The software was not properly installed	Reinstall the software following the specifications on the website for your computer
	The computer does not have the basic requirements necessary	Be sure that your computer has, at the very least, an Intel Celeron Processor 2.40 GHz, 256 MB RAM, 20 GB hard drive and FireWire port
The laser will not activate	The power is 'OFF'	Turn the laser on; make sure the safety keys are initiated
	The power source is depleted	Change the batteries in the laser
	The laser has exceeded its lifetime	Check the laser's lifetime against its logged hours of use; replace or refurbish the laser if necessary
The laser beam does not pass through the HARV	The precision mirror is not properly aligned	Align the mirror at a 45° angle of reflectance from the laser sight and the HARV
The cells will not proliferate	The cells are not viable	Be sure the cells are proliferating, validating their viability

TABLE 1 | Troubleshooting table (continued).

Problem	Possible reason	Solution
	The cells were removed from the incubator too long	Be sure to either create an experiment that does not deteriorate the cell's viability or place the system in an incubator
	The culture medium has expired or is contaminated	Be sure to check the expiration date of the medium and its effect on cell proliferation
	The incubator is malfunctioning	Check all connections to the incubator, the CO_2 level, all tubing and the incubator power. Be sure to address any alarms
The HARV has become contaminated	The HARV was not properly sterilized after inoculation	Use a new HARV or sterilize a previously used HARV with NaOH prior to running an experiment. Rinse the HARV with 70% ethanol following inoculation
	Sterile technique was not followed	Use sterile technique throughout the inoculation, being sure not to put foreign substances into the HARV
	The aseptic hood is malfunctioning	Make sure that the blower of the hood is on and that the surfaces inside the environment are free from contamination
The HARV is losing volume	The ports have not been locked	Be sure that the locks are turned to their locking angles as not to drain the HARV during rotation. Make sure that the HARV is not leaking or damaged (perhaps due to too much medium in the HARV)

ANTICIPATED RESULTS

In vitro imaging and analysis with these horizontal microscope systems will provide dynamic data on aggregation kinetics of various cell types as they proliferate and form 3D aggregates. Also, these images will yield insights into the principles and practices of bioreactor trajectories, which is an important part of our attempts to optimize the reproducible generation of standardized aggregates (**Fig. 8**). Our recent publication is based on these real-time systems and validates the size specifications of the manufacturer's calibration beads, the experimentally measured diameters of PC12 cells[14,24] (**Fig. 9**), and the numerical trajectory theory proposed by earlier models[12,13] (**Fig. 3**). Also, images provided by the system have been compared across different cell lines for aggregation characteristics between 2D tissue growth and 3D tissue growth (G.P.B., Manolya Eyiyurekli, David Breen and P.I.L., unpublished results).

Most techniques for growing tissue in 3D have been static endpoint measurements, which are intrinsically invasive and destructive to the nascent tissue. So, the process of stopping the RWV to remove aliquots of nascent organoids from their proliferative environment causes shear forces that are destructive to delicate cell-cell adhesions. With the advent of this system, real-time dynamic imaging provides the clear capability to study the growth of more native tissue in its 'natural' environment over time (**Fig. 10**).

ACKNOWLEDGMENTS The authors would like to gratefully thank Ken Urish at the University of Pittsburgh for his assistance in modeling the intelligent-feedback system.

COMPETING INTERESTS STATEMENT The authors declare that they have no competing financial interests.

Published online at http://www.natureprotocols.com
Reprints and permissions information is available online at http://npg.nature.com/reprintsandpermissions

1. Granet, C., Laroche, N., Vico, L., Alexandre, C. & Lafage-Proust, M.H. Rotating-wall vessels, promising bioreactors for osteoblastic cell culture: comparison with other 3D conditions. *Med. Biol. Eng. Comp.* **36**, 513–519 (1998).
2. Klement, B.J., Young, Q.M., George, B.J. & Nokkaew, M. Skeletal tissue growth, differentiation, and mineralization in the NASA rotating wall vessel. *Bone* **34**, 487–498 (2004).
3. Lelkes, P.I., Galvan, D.L., Hayman, G.T., Goodwin, T.J., Chatman, D.Y., Cherian, S., Garcia, R.M. & Unsworth, B.R. Simulated microgravity conditions enhance differentiation of cultured PC12 cells towards the neuroendocrine phenotype. *In Vitro Cell. Dev. Biol. Animals* **34**, 316–325 (1998).
4. Sanford, G.L., Ellerson, D., Melhado-Gardner, C., Sroufe, A.E. & Harris-Hooker, S. Three-dimensional growth of endothelial cells in the microgravity-based rotating wall vessel bioreactor. *In Vitro Cell. Dev. Biol. Animals* **38**, 493–504 (2002).
5. DiLoreto, S., Sebastiani, P., Benedetti, E., Zimmitti, V., Caracciolo, V., Amicarelli, F., Cimini, A. & Adorno, D. Transient maintenance in bioreactor improves health of neuronal cells. *In Vitro Cell. and Dev. Biol. Animals* **42**, 134–142 (2006).
6. Johanson, K., Allen, P.L., Gonzalez-Villalobos, R.A., Baker, C.B., D'Elia, R. & Hammond, T.G. Gene expression and survival changes in Saccharmyces cerevisiae during suspension culture. *Biotech. Bioeng.* **93**, 1050–1059 (2006).
7. Nickerson, C.A., Ott, M.C., Wilson, J.W., Ramamurthy, R. & Pierson, D.L. Microbial responses to microgravity and other low-shear environments. *Microbiol. Mol. Biol. Rev.* **68**, 345–361 (2004).
8. Low, H.P., Savarese, T.M. & Schwartz, W.J. Neural precursor cells form rudimentary tissue-like structures in a rotating-wall vessel bioreactor. *In Vitro Cell. Dev. Biol. Animals* **22**, 141–147 (2001).
9. Gao, H., Ayyaswamy, P.S. & Ducheyne, P. Dynamics of a microcarrier particle in the simulated microgravity environment of a rotating wall vessel. *Micrograv. Sci. Tech.* **10**, 154–165 (1997).
10. Muhitch, J.W., O'Connor, K.C., Blake, D.A., Lacks, D.J., Rosenzweig, N. & Spaulding, G.F. Characterization of aggregation and protein expression of bovine

corneal endothelial cells as microcarrier cultures in a rotating wall vessel. *Cytotech.* **32**, 253–263 (2000).
11. Smoluchowski, M.V. Versuch einer mathematischen theorie der koagulationskinetik kolloider loesungen. *Z. Phys. Chem* **92**, 129–168 (1917).
12. Pollack, S.R., Meaney, D.F., Levine, E.M., Litt, M. & Johnston, E.D. Numerical model and experimental validation of microcarrier motion in a rotating bioreactor. *Tissue Eng.* **6**, 519–530 (2000).
13. Qiu, Q.Q., Ducheyne, P. & Ayyaswamy, P.S. Fabrication, characterization, and evaluation of bioceramic hollow microspheres used as microcarriers for 3D bone tissue formation in rotating bioreactors. *Biomaterials* **20**, 989–1001 (1999).
14. Manley, P. & Lelkes, P.I. A novel real-time system to monitor cell aggregation and trajectories in rotating wall vessel bioreactors. *J. Biotech.* **125**, 416–424 (2006).
15. Duke, P.J., Danne, E.L. & Montufar-Solis, D. Studies of chondrogenesis in rotating systems. *J. Cell. Biochem.* **51**, 274–282 (1993).
16. Chopra, V., Dinh, T.V. & Hannigan, E.V. Three-dimensional endothelial-tumor epithelial cell interactions in human cervical cancers. *In Vitro Cell. Dev. Biol. Animals* **33**, 432–442 (1997).
17. Lin, H.J., O'Shaughnessy, T.J., Kelly, J. & Ma, W. Neural stem cell differentiation in a cell-collagen-bioreactor culture system. *Brain Res. Dev. Brain Res.* **153**, 163–173 (2004).
18. Wang, X., Wei, G., Yu, W., Zhao, Y., Yu, X. & Ma, X. Scalable producing embryoid bodies by rotary cell culture system and constructing engineered cardiac tissue with ES-derived cardiomyocytes in vitro. *Biotech. Progress* **22**, 811–818 (2006).
19. Goldwasser, S.M. Dissection of a Green Laser Pointer. *Sam's Laser FAQ* 〈http://www.repairfaq.org/sam/lasersam.htm〉 (2006).
20. Lelkes, P.I. & Unsworth, B.R. Neuroectodermal Cell Culture: Endocrine Cells. *Methods Tissue Eng.* 371–382 (2001).
21. Lelkes, P.I., Unsworth, B.R., Saporta, S., Cameron, D.F. & Gallo, G. Culture of Neuroendorcrine and Neuronal Cells for Tissue Engineering. *Cult. Cell. Tissue Eng.* **14**, 375–416 (2006).
22. Lelkes, P.I. & Miller, I.R. Perturbations of membrane structure by optical probes. I. Location and structural sensitivity of merocyanine 540 bound to phospholipid membranes. *J. Memb. Biol.* **52**, 1–15 (1980).
23. NIH *ImageJ Documentation* 〈http://rsb.info.nih.gov/ij/docs/index.html〉 (2006).
24. Fujita, K., Lazarovici, P. & Guroff, G. Regulation of the differentiation of PC12 pheochromocytoma cells. *Environ. Health Perspect.* **80**, 127–142 (1989).
25. Manely, P. & Lelkes, P.I. A novel real-time system to monitor cell aggregation and trajectories in rotating wall vessel bioreactors. *Biotech.* **125**, 416–424 (2006).

Erratum: Real-time assessment of three-dimensional cell aggregation in rotating wall vessel bioreactors *in vitro*

Gregory P Botta, Prakash Manley, Steven Miller and Peter I Lelkes

Nat. Protocols doi:10.1038/nprot.2006.311; published online 14 December; corrected online 4 January 2007.

A duplicate of this article was initially published online 7 December 2006. The correct publication date is 14 December 2006. Also, the footer of the 14 December 2006 PDF version reads "Vol. 1 No. 5" instead of "Vol. 1 No. 4". This error has been corrected in the PDF version of the article.